




# FrzS acts as a polar beacon to recruit SgmX, a central activator of type IV pili during *Myxococcus xanthus* motility

Sarah Bautista<sup>1</sup>, Victoria Schmidt<sup>2</sup>, Annick Guiseppi<sup>1</sup>, Emilia M F Mauriello<sup>1</sup> , Bouchra Attia<sup>2</sup>, Latifa Elantak<sup>2</sup> , Tâm Mignot<sup>1,\*</sup>  & Romain Mercier<sup>1,\*\*</sup> 

## Abstract

In rod-shaped bacteria, type IV pili (Tfp) promote twitching motility by assembling and retracting at the cell pole. In *Myxococcus xanthus*, a bacterium that moves in highly coordinated cell groups, Tfp are activated by a polar activator protein, SgmX. However, while it is known that the Ras-like protein MglA is required for unipolar targeting, how SgmX accesses the cell pole to activate Tfp is unknown. Here, we demonstrate that a polar beacon protein, FrzS, recruits SgmX at the cell pole. We identified two main functional domains, including a Tfp-activating domain and a polar-binding domain. Within the latter, we show that the direct binding of MglA-GTP unveils a hidden motif that binds directly to the FrzS N-terminal response regulator (CheY). Structural analyses reveal that this binding occurs through a novel binding interface for response regulator domains. In conclusion, the findings unveil the protein interaction network leading to the spatial activation of Tfp at the cell pole. This tripartite system is at the root of complex collective behaviours in this predatory bacterium.

**Keywords** cell motility; CheY domain; *Myxococcus xanthus*; response regulator domain; type IV pili

**Subject Categories** Cell Adhesion, Polarity & Cytoskeleton; Microbiology, Virology & Host Pathogen Interaction

**DOI** 10.15252/emboj.2022111661 | Received 13 May 2022 | Revised 17 October 2022 | Accepted 19 October 2022 | Published online 8 November 2022

**The EMBO Journal (2023) 42: e111661**

## Introduction

Type IV pili (Tfp) are broadly distributed molecular machineries in monoderm and diderm bacteria as well as in Archaea, fulfilling numerous cellular functions, such as adhesion to host cells, the import of extracellular DNA (competence), cell–cell interactions and cell motility (Twitching; Giltner *et al.*, 2012; Berry & Pelicic, 2015; Adams *et al.*, 2019). Tfp of the A subclass (discussed herein, Tfpa)

commonly assemble  $\mu\text{m}$ -long filaments by polymerization of pilin (PilA) sub-units from the bacterial inner membrane (IM) that extrude, attach to surfaces and other cells and subsequently retract via the activity of extension (PilB) and retraction motors (PilT; Giltner *et al.*, 2012; Berry & Pelicic, 2015; Gold *et al.*, 2015; Chang *et al.*, 2016, 2017). In diderm bacteria, Tfp basal machineries are assembled from up to nine proteins to span all layers of the cell envelope, in particular, access to the extracellular space requires secretins in the bacterial outer membrane (OM; Chang *et al.*, 2016).

One Tfp key function of Tfpa is to promote motility that can lead to the remarkable formation of coordinated cell groups (called social motility, where hundreds of cells move in a cooperative manner similar to swarming motility in flagellated bacteria; Glog *et al.*, 2013, 2016). At the single-cell level, motility relies on the coordinated action of multiple pilin filaments that literally act as grappling hooks extending outside the envelope and pulling the cell as they retract (Skerker & Berg, 2001; Tala *et al.*, 2019; Mercier *et al.*, 2020). While the basal Tfpa machineries are assembled at the two cell poles in most rod-shaped bacteria (Bhaya *et al.*, 2000; Bulyha *et al.*, 2009; Carter *et al.*, 2017; Nakane & Nishizaka, 2017), motility depends on pole-specific activation mechanisms to promote directional movements (Skerker & Berg, 2001; Tala *et al.*, 2019; Mercier *et al.*, 2020). Thus, molecular mechanisms must take place to promote the unipolar activation of Tfpa machines, a phenomenon not fully understood.

In the model bacteria *Myxococcus xanthus*, motility plays a crucial role to swarm, predate on prey bacteria and build differentiated multicellular structures (fruiting bodies; Mercier & Mignot, 2016). *Myxococcus xanthus* cells can move using two different motility engines, Type-IV pili as mentioned above, which promote the movement of large cell groups (Sun *et al.*, 2000) and the Agl-Glt complex, also called the adventurous motility system, which forms intracellular trafficking complexes that propel the cell as they travel helically along the cell axis and adhere to the surface, forming the so-called focal adhesions (FAs; Faure *et al.*, 2016). Remarkably, both motility engines are activated at one cell pole (herein the leading cell pole), which is controlled by a single-pole-specific activator, the Ras-like

<sup>1</sup> Laboratoire de Chimie Bactérienne, Institut de Microbiologie de la Méditerranée, Aix-Marseille Université-CNRS (UMR7283), Marseille, France

<sup>2</sup> Laboratoire d'Ingénierie des Systèmes Macromoléculaires, Institut de Microbiologie de la Méditerranée, Aix-Marseille Université-CNRS (UMR7255), Marseille, France

\*Corresponding author. Tel: +33 491164592; E-mail: tmignot@imm.cnrs.fr

\*\*Corresponding author. Tel: +33 491164506; E-mail: rmercier@imm.cnrs.fr

G-protein MglA. When complexed with GTP, MglA localizes at the leading cell pole. This asymmetric distribution is promoted by the opposing actions of first, the RomRX complex, a composite guanine exchange factor (GEF) that loads MglA with GTP at the leading cell pole (Szadkowski *et al.*, 2019); and second of MglB, a GTPase-activating protein (GAP) that deactivates MglA by provoking GTP hydrolysis at the opposite cell pole (the lagging pole; Leonardy *et al.*, 2010; Zhang *et al.*, 2010). Importantly, this polarity axis formed by MglA, RomRX and MglB can be rapidly switched to the opposite cell pole by the action of the bacterial chemosensory-like apparatus (Frz system), which leads to a rapid change in the direction of movement (reversals; Guzzo *et al.*, 2018). In the process, MglA is responsible for the activation of both the A- and S-motility systems at the opposite cell pole. How it does so at the molecular level is the topic of this manuscript.

At this stage, the mechanisms appear specific for each motility system. In the case of the Agl-Glt complex, MglA-GTP promotes the assembly of a cytosolic platform formed by the MreB actin cytoskeleton and the AglZ protein (Treuner-Lange *et al.*, 2015; Fu *et al.*, 2018). How this platform interacts with the trans-envelope Agl-Glt proteins remains to be discovered. Somewhat differently, polar activation of the S-motility system by MglA requires the TfpA activator SgmX, a multidomain protein containing 14 tandem repeats of tetratricopeptide repeat (TPR) domains (Mercier *et al.*, 2020; Potapova *et al.*, 2020). MglA-GTP recruits SgmX directly, binding to a motif formed by three consecutive C-terminal TPR domains in the SgmX proteins. This binding unfolds an SgmX polar-binding motif which when recruited by an unknown target allows SgmX to activate TfpA function (Mercier *et al.*, 2020).

In this study, we aimed to discover the mechanism of SgmX polar localization and TfpA activation. We first mapped domains in the SgmX protein and exposed two additional functional motifs in addition to the MglA-binding site (M-domain): one mediating activation of TfpA function (TA-domain or TAD) and the second promoting the anchoring of SgmX at cell poles (S-domain). We then discovered that the polar protein, FrzS protein (Ward *et al.*, 2000), functions as a molecular beacon to position SgmX at the pole. In this process, FrzS and SgmX bind via an interaction between the SgmX S-domain and the FrzS N-terminal response regulator (CheY) domain, addressing the TA-domain to the Tfp complex. Interestingly, while the interaction involved the canonical  $\alpha$ 4-helix of the CheY domain, the interaction interface is novel for a RR protein. Last, we discuss how these findings might explain how MglA activates A- and S-motility separately via the paralogous FrzS and AglZ proteins (Guzzo *et al.*, 2015).

## Results

### The TfpA activator SgmX protein is a three-functional domain protein

The SgmX protein is composed of 14 TPR motifs (Fig 1A; Mercier *et al.*, 2020). We previously demonstrated that the C-terminal TPRs12–14 formed an interaction domain with MglA<sup>GTP</sup>, which is essential for SgmX polar localization (Fig 1A, M Domain; Mercier *et al.*, 2020). However, we observed that SgmX lacking the M-domain localizes to both cell poles, demonstrating that the M-

domain is not *per se* required for polar localization but required for the regulation of unipolar localization by MglA (Fig 1A and B, 2 and see below; Mercier *et al.*, 2020). Therefore, we previously proposed that MglA<sup>GTP</sup> binding to the M-domain could unmask an as-yet-uncharacterized polar targeting domain within SgmX (Mercier *et al.*, 2020).

To precisely delineate this domain, we systematically deleted TPRs of SgmX and analysed how the deletions affected both the polar localization and function of SgmX. We previously showed that expression of SgmX<sup>ΔTPR12–14</sup> (SgmX<sup>mimB</sup>) leads to bipolar localization and decreased S-motility (Fig 1A–C, 2), compared to an SgmX full length that showed a unipolar profile (Fig 1A–C, 1; Mercier *et al.*, 2020). In contrast, SgmX<sup>ΔTPR11–14</sup> that lacks one additional TPR motif (TPR11) is no longer localized at cell poles, which correlated with a complete loss of S-motility (Fig 1A–C, 3), thus suggesting that TPR11 motif is involved in polar binding of SgmX. Because TPR motifs generally form functional domains when associated in a triad (Perez-Riba & Itzhaki, 2019), we expressed an SgmX version that only contained the TPRs9–11 together with the MglA-binding domain (SgmX<sup>ΔTPR1–8</sup>, Fig 1A, 4). Remarkably, SgmX<sup>ΔTPR1–8</sup> was able to localize at cell poles but its S-motility function was abolished (Fig 1A–C, 4). Further deletion of the TPR9 motif (SgmX<sup>ΔTPR1–9</sup>) abolished polar localization (Fig 1A–C, 5); suggesting that TPRs9–11 formed the polar-binding domain of SgmX, which we directly demonstrated by showing that expression of these motifs alone (SgmX<sup>TPR9–11</sup>) is sufficient for polar localization (Fig 1A–C, 6).

Combined with previous findings, the above results demonstrated that SgmX contained three distinct functional domains that can be uncoupled: (i) a TfpA-activating domain (TAD) formed by the TPRs1–8, (ii) a polar-anchoring domain (S-domain) formed by the TPRs9–11 and (iii) a regulatory domain formed by the TPRs 12–14 (M-domain) and bound by MglA<sup>GTP</sup>.

### The S-motility protein FrzS controls the polar localization of SgmX

We next searched for a potential polar-anchoring factor of SgmX; one protein candidate is the FrzS protein, which was shown to be required for S-motility (Ward *et al.*, 2000). Importantly, FrzS localizes asymmetrically to the cell poles and its dynamics are coupled to reversals in an MglA-dependent manner but its polar localization *per se* is MglA independent (Mignot *et al.*, 2007; Zhang *et al.*, 2012). We therefore tested the potential contribution of FrzS to SgmX localization and function.

The localization of FrzS and SgmX does not strictly overlap: in wild-type cells, FrzS-mcherry shows a bipolar localization profile while SgmX-sfGFP localizes at one cell pole (Fig 2A). However, this is the result of MglA regulation because SgmX<sup>ΔTPR12–14</sup> (SgmX<sup>mimB</sup>; Mercier *et al.*, 2020), which no longer relies on MglA for polar binding, is bipolar and perfectly co-localizes with FrzS-mcherry (Fig 2B). This co-localization could reflect a direct relationship between SgmX and FrzS because neither SgmX nor SgmX<sup>mimB</sup> localized at the cell pole in a strain lacking FrzS (Fig 2C and D). Last, we previously showed that SgmX<sup>mimB</sup> can localize in the absence of MglA and its associated regulators RomR and MglB ( $\Delta$ BAR; Fig EV1A; Mercier *et al.*, 2020). In contrast, FrzS is essential for SgmX<sup>mimB</sup> localization in a  $\Delta$ BAR background as SgmX<sup>mimB</sup>-sfGFP no longer localized at cell poles in a  $\Delta$ BAR  $\Delta$ frzS strain (Fig 2E). Importantly, a  $\Delta$ BAR

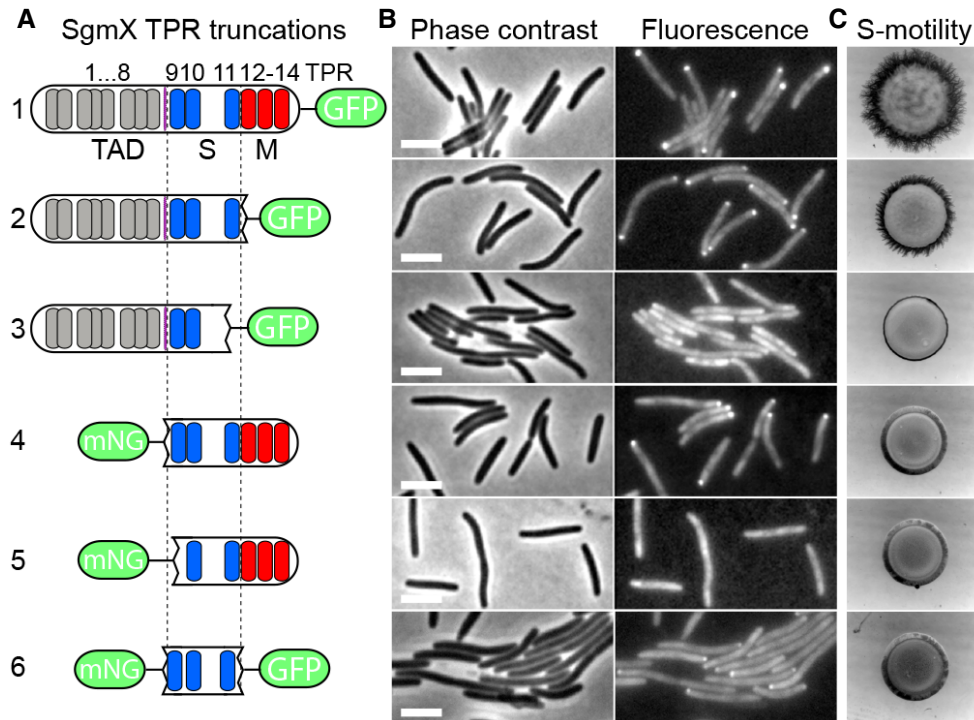


**Figure 1. The SgmX protein domain functions.**

**A** Schematic representation and organization of the 14 tetratricopeptide repeats (TPR) of SgmX (1) and corresponding SgmX truncated variants (2–5). TPRs are represented by different coloured cylinders according to their domain functions. The purple line shows the proline-rich region of SgmX; the fluorophore sfGFP or mNeonGreen (mNG) is represented in green and the dotted line shows the polar bonding domain of SgmX.

**B, C** Fluorescence microscopy images (B) and corresponding motility phenotypic assay (C) of *M. xanthus*  $\Delta$ sgmX strains bearing SgmX (1) or truncated variants of SgmX (2–5) fused to sfGFP or mNeongreen, as represented in (A). Scale bar: 3  $\mu$ m.

$\Delta$ frzS *sgmX*<sup>mmB</sup>-sfGFP strain was non-motile compared to a  $\Delta$ BAR *sgmX*<sup>mmB</sup>-sfGFP, suggesting that loss of polar SgmX<sup>mmB</sup> localization leads to the motility defect (Fig EV1B).

### FrzS regulates SgmX polar localization by a direct interaction

The above results suggest that a function of FrzS is to recruit SgmX at the cell pole following the exposure of the SgmX S-domain by MglA<sup>GTP</sup>. The FrzS protein is composed of three distinct domains (Fig 3A; Mignot et al, 2007): (i) a N-terminal pseudo-receiver, which adopts a typical CheY domain conformation but lost its autophosphorylation capacity (FrzS<sup>CheY</sup>; Fraser et al, 2007), important for motility function (Mignot et al, 2007); (ii) a degenerate DNA-binding domain of unknown function (FrzS<sup>DBD</sup>; Mignot et al, 2007); and (iii) a C-terminal extended coiled-coil domain, sufficient for FrzS polar localization (FrzS<sup>coiled-coil</sup>; Mignot et al, 2007). Therefore, the CheY domain of FrzS might be implicated in motility function by regulating SgmX polar localization. In agreement, whereas an FrzS<sup>A<sup>CheY</sup></sup>-GFP showed a bipolar localization profile similar to FrzS full length, SgmX showed a diffuse localization profile (Fig 3B).

We next determined if FrzS<sup>CheY</sup> was sufficient to localize SgmX at the pole. To test this, we used the natural property of the *Caulobacter crescentus* protein PopZ to localize at bacterial cell poles (Lim & Bernhardt, 2019). In wild-type *M. xanthus* cells, expressing a fusion protein mNeongreen(mNG)-PopZ did not affect S-motility in

comparison to a null-expressing strain (Fig EV2A). Importantly and like in other bacteria such as *Escherichia coli*, mNG-PopZ showed predominantly a unipolar distribution pattern (Figs 3C and D, and EV2B). As expected, the expression of mNG-PopZ in a  $\Delta$ frzS *sgmX*-mcherry strain, neither restored SgmX polar localization (Fig 3D) nor S-motility (Fig 3E). We therefore fused the N-terminal part of FrzS<sup>Nt</sup> (CheY and DBD domains) to the mNG-PopZ protein, and the resulting fusion also showed a polar distribution profile (Fig 3C and D). But contrarily to the mNG-PopZ protein, FrzS<sup>Nter</sup>-mNG-PopZ not only restored the polar distribution of SgmX (Fig 3D) but also S-motility (Fig 3E). We then tested which domain of the FrzS<sup>Nter</sup> recruits SgmX to the pole: expression of an FrzS<sup>CheY</sup>-mNG-PopZ fusion protein showed that the CheY domain of FrzS is sufficient to both restore the SgmX polar localization and the S-motility of a  $\Delta$ frzS *sgmX*-mcherry strain (Fig 3C–E). Remarkably, SgmX also retained its ability to switch poles upon MglA-dependent cellular reversion (Fig EV2C and Movie EV1).

We then characterized if FrzS<sup>CheY</sup> and SgmX interact directly. To do so, we recapitulated the PopZ protein localization assay in *E. coli* where possible intermediates partners should be missing. Like in *M. xanthus*, GFP-PopZ<sup>H3H4</sup> fusion protein showed polar localization when expressed together with PopZ in *E. coli* (Fig 3F; Lim & Bernhardt, 2019). Importantly, the SgmX-mcherry protein fusion showed a diffuse localization profile in GFP-PopZ<sup>H3H4</sup>-expressing cells (Fig 3F). In contrast, a polar localization of SgmX-mcherry was

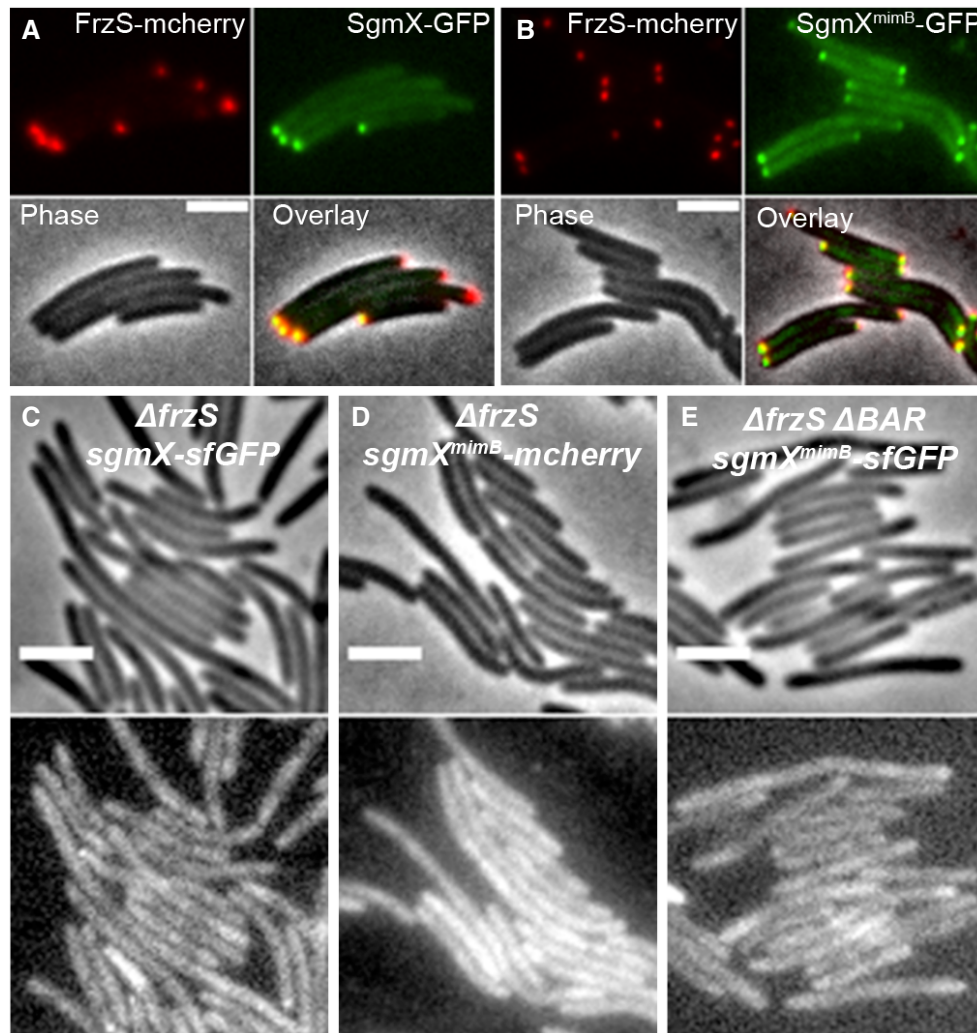


**Figure 2. FrzS regulates SgmX polar localization.**

A, B Epifluorescence (FrzS-mcherry and SgmX-sfGFP or SgmX<sup>mimB</sup>-sfGFP), phase contrast (Phase) and corresponding overlay (Overlay) images of the colocalization of FrzS-mcherry bi-polar foci with SgmX-sfGFP (A) of the strain RM498 (*frzS-mcherry sgmX-sfGFP*) or with SgmX<sup>mimB</sup>-sfGFP (B) of the strain RM499 (*frzS-mcherry sgmX<sup>mimB</sup>-sfGFP*). Scale bar: 3  $\mu$ m.

C–E Phase-contrast (top) and corresponding epifluorescence (bottom) images of strains RM300 ( *$\Delta$ frzS sgmX-sfGFP*, C), RM501 ( *$\Delta$ frzS sgmX<sup>mimB</sup>-sfGFP*, D) and RM288 ( *$\Delta$ frzS  $\Delta$ BAR sgmX<sup>mimB</sup>-sfGFP*, E). Scale bar: 3  $\mu$ m.

observed when it was expressed together with the FrzS<sup>CheY</sup>-GFP-PopZ<sup>H13H4</sup> fusion (Fig 3G), strongly suggesting that FrzS-mediated SgmX polar localization is mediated via a direct interaction.

#### SgmX binds to FrzS via a non-canonical interface of the FrzS CheY domain

The CheY domain of FrzS is among a growing number of poorly characterized family of pseudo-receiver domain proteins that adopt CheY-like conformations but do not depend on phosphorylation to fulfil their output function (Bourret, 2010; Collins & Childers, 2021). In FrzS, key phosphorylation residues such as Asp13 and Asp12, as well as the conserved transducing Thr87, are missing, which was shown to prevent a phosphorylation-dependent conformational switch (Fraser *et al*, 2007). Nevertheless, the output face, and in

particular the key Tyr102, is conserved and critical for function, suggesting that FrzS<sup>CheY</sup> interacts with its target(s) in a somewhat canonical manner (Fraser *et al*, 2007). Thus, to get molecular insights into the FrzS<sup>CheY</sup> and SgmX interaction, we mapped the SgmX-FrzS<sup>CheY</sup> interaction interface by NMR spectroscopy (Fig 4). The FrzS<sup>CheY</sup> 2D <sup>1</sup>H, <sup>15</sup>N HSQC spectra showed a similar profile as previously described with sharp and well-dispersed peaks (Fraser *et al*, 2007; Fig 4A, purple and Appendix Fig S1). In the presence of SgmX, several FrzS<sup>CheY</sup> resonances were perturbed on the 2D-HSQC spectra (chemical shift variations: and peak intensity decrease; Fig 4A, green), thus confirming their direct interaction. We next assigned the FrzS<sup>CheY</sup> NMR resonances to identify FrzS<sup>CheY</sup> amino acids that become perturbed upon SgmX binding (Fig 4A and Appendix Fig S1) and report them on the available FrzS<sup>CheY</sup> structure (Fraser *et al*, 2007; Fig 4B and C). Remarkably, one of the most

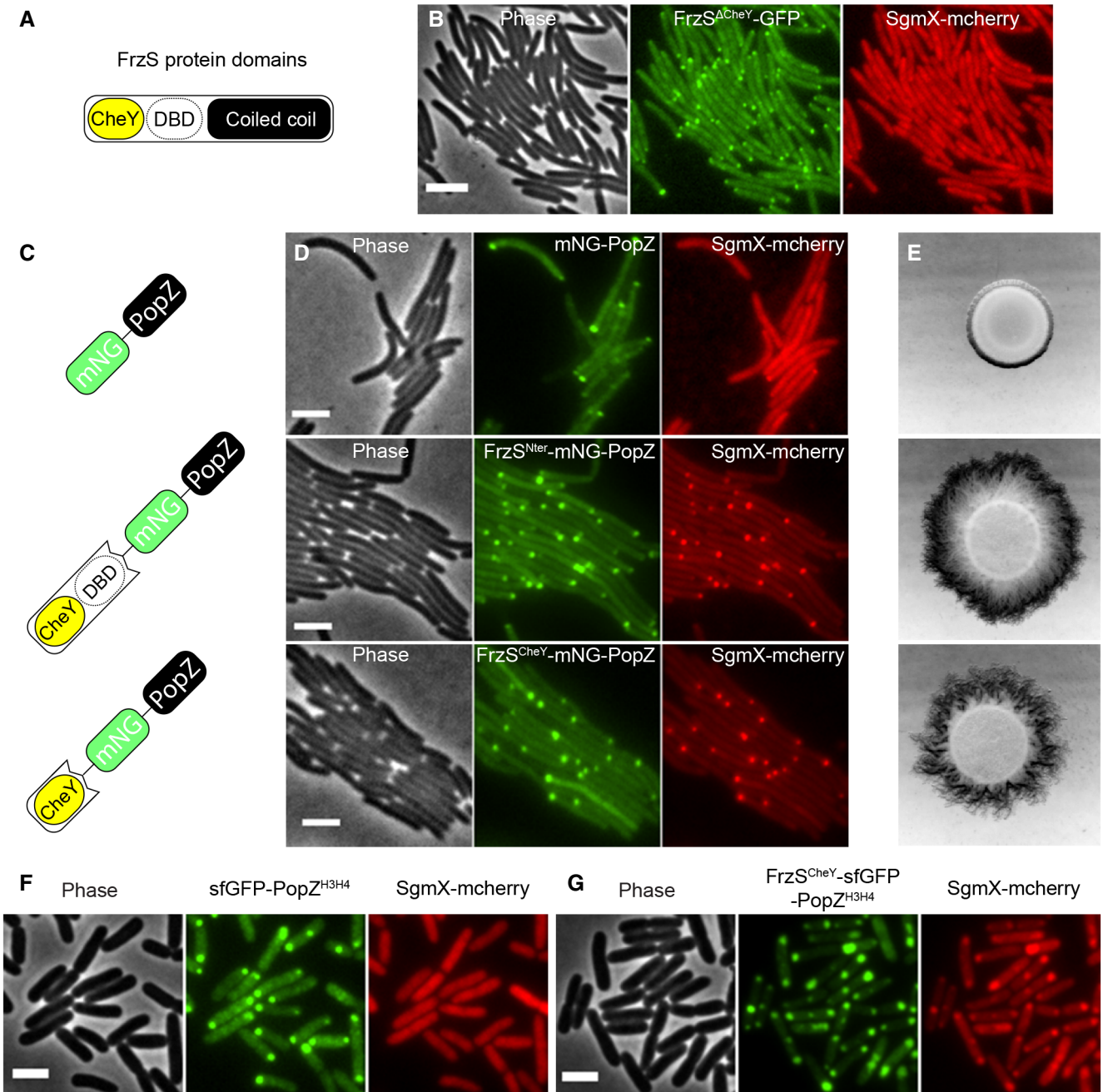


**Figure 3. The response regulator of FrzS interacts directly with SgmX.**

- A Schematic representation of the *M. xanthus* FrzS protein composed of three distinct domains: (i), an N-terminal pseudo-receiver (CheY, Yellow), (ii), a degenerate DNA-binding domain (DBD) and (iii), a C-terminal extended coiled-coil domain (coiled-coil, Black).
- B Phase-contrast (Phase) and epifluorescence (mNG-PopZ and SgmX-mcherry) images of the localization of SgmX-mcherry in *M. xanthus* cells of the strain RM504 (*frzS*<sup>ΔCheY</sup>-GFP *sgmX*-mcherry) expressing FrzS<sup>ΔCheY</sup>-GFP (Scale bar: 4 μm).
- C Schematic representation of protein fusions created between different domains of FrzS from (A) and the PopZ protein. The mNG and PopZ proteins are represented by green and black circles respectively.
- D Phase-contrast (Phase) and epifluorescence (mNG-PopZ and SgmX-mcherry) images of the localization of SgmX-mcherry in *M. xanthus* cells of strains RM479 (*AfrzS* *sgmX*-mcherry *attMx8*:: *P*<sub>pilA</sub>-mNG-popZ, Top), RM502 (*AfrzS* *sgmX*-mcherry *attMx8*:: *P*<sub>pilA</sub>*AfrzS*<sup>Nter</sup>-mNG-popZ, middle) and RM484 (*AfrzS* *sgmX*-mcherry *attMx8*:: *P*<sub>pilA</sub>-*frzS*<sup>CheY</sup>-mNG-popZ, bottom) expressing various chimeric PopZ fusion presented in (A) (Scale bar: 3 μm).
- E Motility phenotypic assay of strains RM479 (*AfrzS* *sgmX*-mcherry *attMx8*:: *P*<sub>pilA</sub>-mNG-popZ, Top), RM502 (*AfrzS* *sgmX*-mcherry *attMx8*:: *P*<sub>pilA</sub>-*frzS*<sup>Nter</sup>-mNG-popZ, middle) and RM484 (*AfrzS* *sgmX*-mcherry *attMx8*:: *P*<sub>pilA</sub>-*frzS*<sup>CheY</sup>-mNG-popZ, bottom) expressing various chimeric PopZ fusion presented in (A).
- F, G Phase-contrast (Phase) and epifluorescence images of the localization of SgmX-mcherry in *E. coli* cells of strains RM<sub>ec</sub>269 (*lacI*<sup>q</sup> *P*<sub>lac</sub>-*sgmX*-mcherry *P*<sub>Bad</sub> sfGFP-H3-H4<sup>PopZ</sup>, F) or RM<sub>ec</sub>270 (*lacI*<sup>q</sup> *P*<sub>lac</sub>-*sgmX*-mcherry *frzS*<sup>CheY</sup>-sfGFP-H3-H4<sup>PopZ</sup>, G) expressing PopZ sfGFP-H3-H4<sup>PopZ</sup> or PopZ FrzS<sup>CheY</sup>-sfGFP-H3-H4<sup>PopZ</sup> respectively (Scale bar: 3 μm).

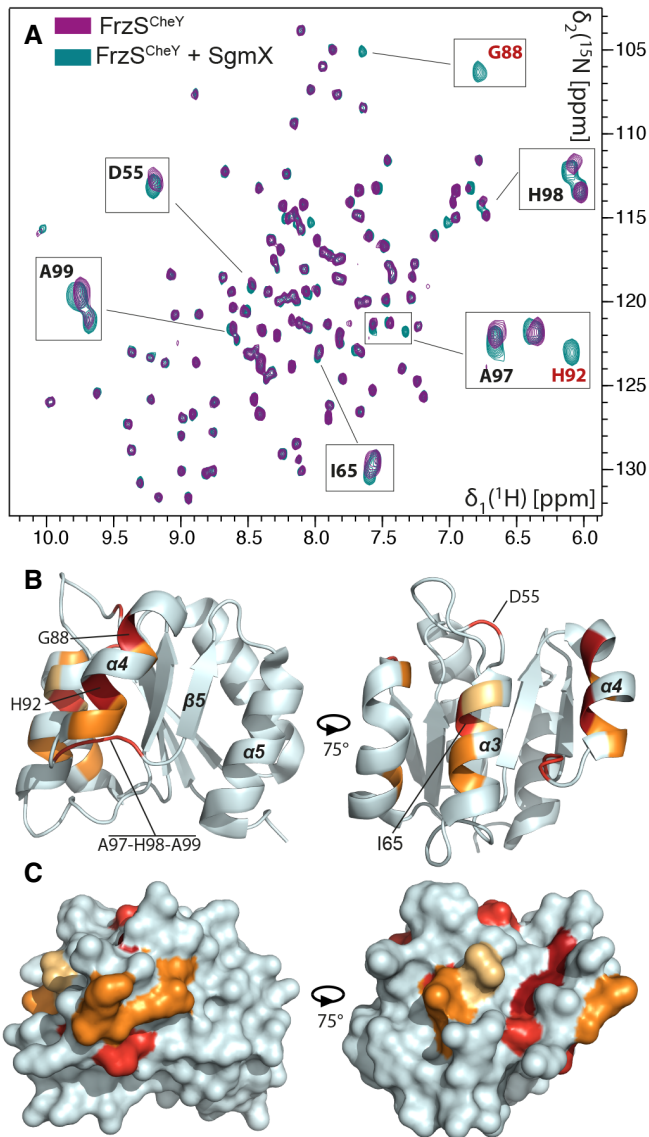


**Figure 4. NMR spectroscopy of FrzS<sup>CheY</sup> upon SgmX interaction.**

- A Superposition of 2D <sup>1</sup>H, <sup>15</sup>N HSQC spectrum of 0.10 mM <sup>15</sup>N-labelled FrzS<sup>CheY</sup> in the absence (teal) and in the presence of SgmX (purple) recorded at 298 K in 50 mM Tris pH 7.2 with 150 mM NaCl and 5 mM MgCl<sub>2</sub> in 95%/5% D<sub>2</sub>O. Expanded regions show FrzS<sup>CheY</sup> resonances representative of those that showed large CSPs on binding to SgmX.
- B, C Chemical shift perturbations upon SgmX interaction are mapped onto cartoon (B) or surface (C) representation of the FrzS<sup>CheY</sup> structure (PDB ID: 2GKG (Fraser *et al.*, 2007)) from orange (significant perturbations, above 2σ from the average Δδ and I/I<sub>0</sub>) to red (highest perturbations). Labels identify residues with the highest perturbations. Two views of the FrzS structure representation are shown.

perturbed residues upon SgmX interaction is H92 on helix α4 which has been previously shown to be essential for S-motility (Fraser *et al.*, 2007). In the canonical phosphorylated receiver domain (RD), the output face α4-β5-α5 forms the interaction interface with effectors (Gao & Stock, 2010). Here, important chemical shift perturbations observed on FrzS<sup>CheY</sup> upon SgmX interactions are clustered

along the α4 helix but also on the adjacent loop with amino acids A97-H98-A99 (Fig 4B and Appendix Fig S1). Interestingly, no chemical shift perturbations could be observed on neither the β5 strand nor the α5 helix (Fig 4B and Appendix Fig S1). In contrast, the resonance of residues clustered along the α3 helix was chemically shifted (Fig 4B and Appendix Fig S1). This second interaction patch on the α3 helix suggests that the α3-β4-α4 surface forms the SgmX output face instead of the canonical α4-β5-α5 surface (Fig 4C).

To validate the characterized FrzS<sup>CheY</sup>-SgmX output face, we generated different FrzS<sup>CheY</sup> mutants and tested their interaction with SgmX by NMR (Fig EV3). We generated the amino acids substitutions mutants FrzS<sup>CheY</sup>-H92A, FrzS<sup>CheY</sup>-G88A and FrzS<sup>CheY</sup>-AHA(97-99)GGG that all showed strong chemical shift perturbations upon SgmX interaction (Fig 4A and Appendix Fig S1). Importantly, all generated FrzS<sup>CheY</sup> mutants showed well-resolved spectra demonstrating that the introduced mutations did not affect the structural integrity of the mutated domain (Fig EV3, teal). Remarkably, no chemical shift perturbations could be further observed in all the tested FrzS<sup>CheY</sup> mutants upon SgmX interaction (Fig EV3, purple). Therefore, this strongly supports the idea that these amino acids are involved in the interaction. Thus, it is striking that in the FrzS pseudo-receiver domain, an interface distinct from that which normally undergoes a conformational change upon phosphorylation in canonical receiver domains has been selected for interaction with SgmX (Bourret, 2010).

#### FrzS<sup>CheY</sup> and SgmX interaction is not required for TfpA activation

The results above suggest that the sole function of the CheY domain of FrzS is to recruit SgmX, targeting the SgmX<sup>TAD</sup> to the pole where it activates Tfp, rather than regulating Tfp function itself. If so, a chimeric fusion between the SgmX<sup>TAD</sup> and FrzS<sup>coiled coil</sup> domains (Fig 5A) should be sufficient to localize SgmX<sup>TAD</sup> at the cell pole and restore TfpA-dependant S-motility in the absence of the CheY domain of FrzS. As expected, and like the full-length FrzS protein, the chimera showed a bipolar localization profile (Fig 5B). Importantly, we could observe S-motility resumption when the chimera was expressed in a *frzs sgmX* deletion strain (Fig 5C), showing that neither the CheY domain of FrzS nor its interaction with SgmX are directly implicated in TfpA activation. Ultimately, the above result also suggests that FrzS *per se* might also be dispensable provided that any given polar module localizes SgmX at the cell pole. To test this hypothesis, we expressed an SgmX-PopZ or SgmX<sup>TAD</sup>-PopZ fusion protein in a *frzs* mutant (Fig 5D). Remarkably, the expression of both fusions restored not only the polar localization of SgmX but also S-motility; as expected, polar localization or S-motility was not restored in the absence of PopZ (Fig 5E and F). Thus, altogether, the above results demonstrate that the function of FrzS is to act as a molecular beacon, positioning SgmX at the cell poles, which in turn activates TfpA activation.

## Discussion

### FrzS<sup>CheY</sup> is a docking domain for SgmX

CheY-like pseudo-receiver domains that exert their function independently of phosphorylation are emerging in a number of proteins

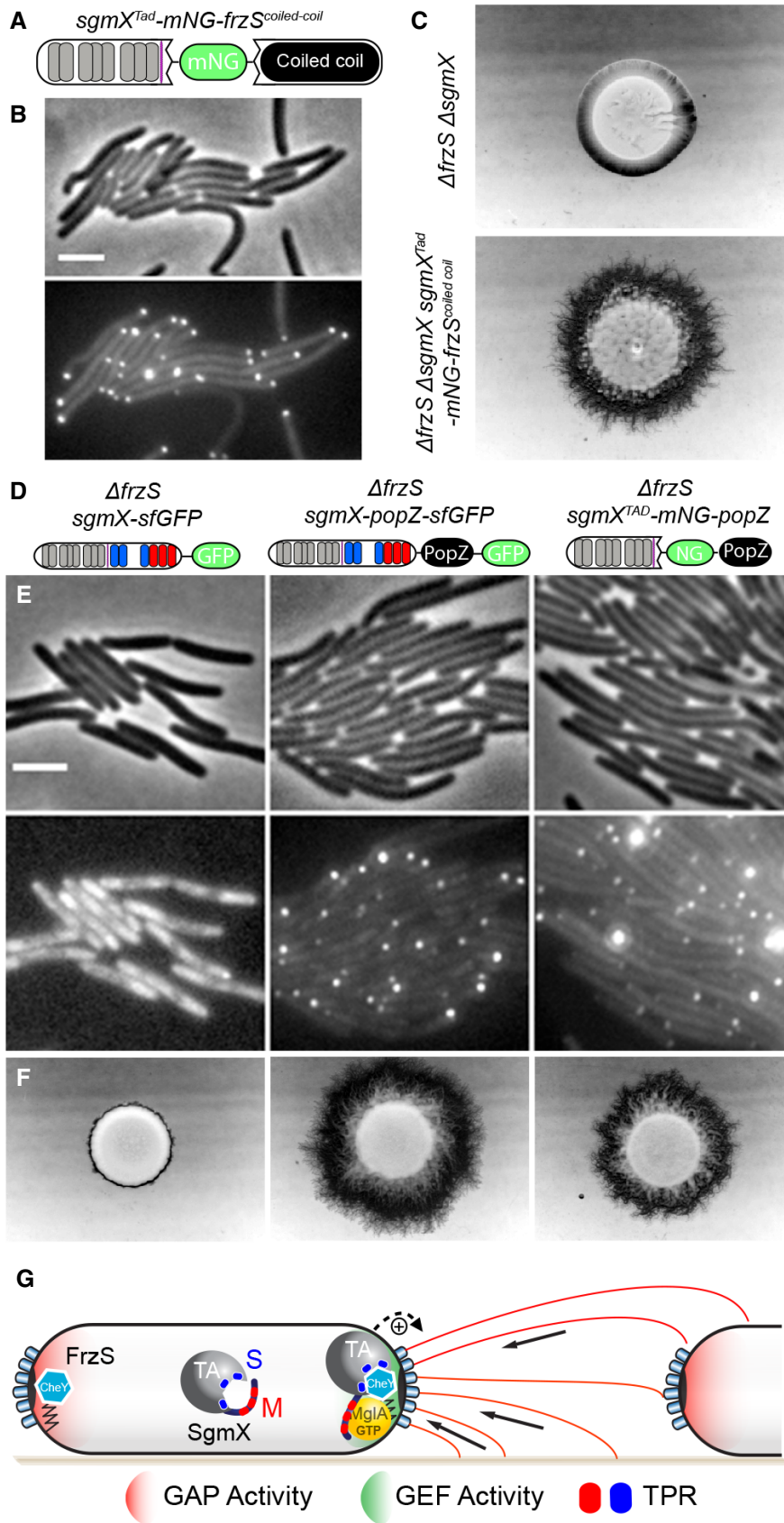


Figure 5.

**Figure 5. The FrzS protein works as a polar-anchoring factor for SgmX.**

- A Schematic representation of the protein fusion between SgmX<sup>TAD</sup> and FrzS<sup>coiled-coil</sup> domains.
- B Phase-contrast (Phase) and epifluorescence images of *M. xanthus* cells expressing SgmX<sup>TAD</sup>-mNG-FrzS<sup>coiled-coil</sup> of the strain RM488 (*ΔfrzS ΔsgmX sgmX<sup>TAD</sup>-mNG-FrzS<sup>coiled-coil</sup>*) (Scale bar: 3 μm).
- C Motility phenotypic assay of strains RM437 (*ΔfrzS ΔsgmX*) and RM488 (*ΔfrzS ΔsgmX sgmX<sup>TAD</sup>-mNG-FrzS<sup>coiled-coil</sup>*) on soft agar plate.
- D Schematic representation of protein fusions created between SgmX or SgmX<sup>TAD</sup> and the PopZ protein and expressed in an *frzS* strain. The protein sfGFP or mNG and PopZ proteins are represented by green and black circles respectively.
- E Phase-contrast and epifluorescence images *M. xanthus* cells of strains RM300 (*ΔfrzS sgmX-sfGFP*, left), RM340 (*ΔfrzS sgmX-popZ-sfGFP*, middle) and RM487 (*ΔfrzS ΔsgmX sgmX<sup>TAD</sup>-mNG-popZ*, right) expressing protein fusions from (D). (Scale bar: 3 μm).
- F Motility phenotypic assay of strains RM300 (*ΔfrzS sgmX-sfGFP*, left), RM340 (*ΔfrzS sgmX-popZ-sfGFP*, middle) and RM487 (*ΔfrzS ΔsgmX sgmX<sup>TAD</sup>-mNG-popZ*, right) on soft agar plate.
- G A model for the S-motility activation by the small GTPase MglA in *M. xanthus*. MglA-GTP is asymmetrically localized at the leading pole of the cell (by the combined action of MglB (GAP activity, red) and RomR/X (GEF activity, green)). The SgmX MglA-binding domain (red TPRs) inhibits SgmX polar localization by blocking the SgmX FrzS-binding domain (grey TPRs). Thus, the interaction between MglA-GTP and the SgmX unmasks the FrzS-binding domain of SgmX that tethers SgmX to the pole where it activates Tpa machines via its Tpa-activating domain (TAD).

across bacteria (Bourret, 2010; Collins & Childers, 2021). Little is known about their exact mode of action (Maule *et al*, 2015) and it is often proposed that these pseudo-receiver domains are locked in a state similar to the phosphorylated active state of canonical receiver domains, homodimerizing or interacting with other ligands constitutively (Al-Bassam *et al*, 2014; Desai & Kenney, 2017; Kaczmarczyk *et al*, 2020; Collins & Childers, 2021). Our results demonstrate that the sole function of FrzS<sup>CheY</sup> is to act as a docking domain for SgmX: (i) SgmX and FrzS<sup>CheY</sup> interact directly; (ii) FrzS<sup>CheY</sup> is sufficient to localize SgmX at the cell pole; and (iii) The SgmX-FrzS<sup>CheY</sup> interaction is dispensable for S-motility when SgmX is fused to a polar protein. Thus, our results not only unveiled the FrzS molecular function in *M. xanthus* motility but also characterized the first pseudo-receiver domain protein ligand, here a domain formed by three TPR motifs.

Upon phosphorylation, canonical receiver domains all show similar interaction modes. Typically, the autophosphorylation of the conserved Asp residues leads to the removal of a steric constraint mediated by a bulky residue (typically a tyrosine) that frees the conserved α4-β5-α5 interface for dimerization or interaction with an output protein (Bourret, 2010; Desai & Kenney, 2017; Gao *et al*, 2019). Here, using NMR spectroscopy, we mapped the SgmX surface of interaction on FrzS<sup>CheY</sup> (Fig 4). We firstly showed that the interaction involved the canonical α4 helix (Fig 4). This observation is in agreement with the fact that substitutions along the α4 helix abolished *M. xanthus* S-motility (Fraser *et al*, 2007), probably by blocking the SgmX-FrzS<sup>CheY</sup> interaction. Moreover, NMR spectroscopy also revealed second patches of interaction on the α3 helix (Fig 4). Thus, FrzS<sup>CheY</sup> likely interacts with its partner SgmX with a surface formed by the α3-β4-α4 interface. This is an interesting finding because it suggests that pseudo-receiver domains functioning as docking domains have evolved new modes of interactions to recruit their ligands. It would be interesting to test whether the α3-β4-α4 interface is especially suitable for interaction with TPR domains, such as in SgmX. We are conducting structural studies to explore this possibility.

#### Mechanism for polar localization of SgmX by the combined action of MglA and FrzS

We previously demonstrated that active MglA controlled SgmX polar distribution by a direct interaction with the SgmX M-domain,

composed of the last three TPR motifs at its C-terminus (Fig 1; Mercier *et al*, 2020). Here, we characterized the SgmX S-Domain, composed of three TPR motifs adjacent to the M-domain, which can alone localize at the pole when expressed in *M. xanthus* cells (Fig 1). Furthermore, we identified the response regulator (CheY) domain of the FrzS protein as the binding partner for the SgmX S-domain (Fig 3).

We can now propose a two-step interaction model that dynamically tethers SgmX at the cell pole (Fig 5G):

- i MglA interaction with the SgmX M-domain (Fig 5G, red cylinder) unveils the SgmX S-domain (Fig 5G, blue cylinder), which is otherwise hidden when SgmX is not in a complex with MglA.
- ii FrzS<sup>CheY</sup> then interacts with the SgmX S-domain, anchoring the SgmX<sup>TAD</sup> at the pole where it activates Tpa activity and enables S-motility by a yet unknown mechanism (Fig 5G, blue cylinder).

Remarkably, this regulation by two independent factors not only ensures the unipolar localization of SgmX but also its ability to switch from pole to pole during reversals. In mutants that lack the SgmX M-domain, SgmX is bipolar perfectly matching FrzS bipolar localization. Thus, the function of MglA is to promote SgmX localization at one cell pole only. Indeed, SgmX can switch poles when the FrzS<sup>CheY</sup>-NG-PopZ is expressed in place of FrzS, clearly demonstrating that FrzS docks SgmX at cell poles while MglA dictates which pole should be active.

How the coiled-coil domain of FrzS targets FrzS to the cell pole remains a standing question. FrzS<sup>coiled-coil</sup> could interact with an undefined polar factor or it could also make spontaneous autoassemblies at the cell pole. One way to discriminate between these possibilities could be to express them in heterologous hosts such as *E. coli* and see whether the protein goes to the pole. This is, for example, the case for PopZ. Unfortunately, this cannot be easily done for FrzS because when expressed its coiled-coil domain makes large periodic structures in the *E. coli* cytosol. But it is nevertheless possible that the FrzS coiled-coil domain recognizes the cell pole spontaneously, for example, the *Bacillus subtilis* cell division protein DivIVA self-assembles at the cell pole via the sole action of its coiled-coil domain by sensing the negative curvature of the cell pole (Lenarcic *et al*, 2009; Oliva *et al*, 2010).



## Motility regulation of *M. xanthus* by MglA

We now have a good molecular understanding of the mechanism by which MglA activates S-motility, favouring the polar targeting of the SgmX TAD domain to Tfpas and thus leading to their unipolar activation. The SgmX TAD is sufficient for this activation but the mechanism involved remains to be discovered. PilB motors do not localize at the cell pole in the absence of SgmX (Potapova *et al*, 2020), suggesting that SgmX could favour the insertion of PilB at the pilus base. However, no interaction has yet been described between SgmX TAD and PilB.

Nevertheless, the discovery of FrzS function provides clues to understanding how a single regulator such as MglA activates both the S- and A-motility systems. Quite remarkably, activation of the Agl-Glt machinery at the cell pole depends both on MglA and AglZ, an FrzS paralogue (Guzzo *et al*, 2015), containing both a CheY-like domain and an extended coiled-coil domain (Yang *et al*, 2004). Like FrzS<sup>CheY</sup>, AglZ<sup>CheY</sup> is also predicted to be non-functional for autophosphorylation and AglZ shows a polar distribution in cells, probably also mediated by its coiled-coil domain. This suggests that AglZ might also recruit an MglA-dependent A-motility activator (probably a TPR protein). Phylogenetic studies suggest that the A-motility system was acquired late during the differentiation of the deltaproteobacteria, likely after the emergence of the S-motility system and its regulators MglA, FrzS and SgmX (Guzzo *et al*, 2015; Mercier *et al*, 2020). In fact, AglZ likely emerged following a gene duplication event that might have coincided with the acquisition of the Agl-Glt complex. Thus, the duplication of a single gene and its specialization to distinct motility systems may underlie their branching to a single regulator, here MglA.

## Materials and Methods

### Bacterial strains, plasmids and growth conditions

The bacterial strains and plasmid constructs used in this study are shown in Appendix Tables S1 and S2. A list of primers used in this study is shown in Appendix Table S3. DNA manipulations and *E. coli* transformation were carried out using standard methods (Sambrook *et al*, 1989). All plasmid constructions were verified by Sanger sequencing (Eurofins GATC-Biotech, Germany). Plasmids were introduced in *M. xanthus* by electroporation. Mutants and expression of protein fusions were obtained by the integration—excision recombination method as previously reported (Bustamante *et al*, 2004) or by site-specific integration at the Mx8-phage attachment site (Bustamante *et al*, 2004). *E. coli* cells were grown in Luria–Bertani broth (LB) and on Luria–Bertani 1.5% agar plate. *M. xanthus* DZ2 cells were grown in CYE media (1% (w/v) casitone, 0.5% yeast extract, 10 mM MOPS (pH 7.6) and 4 mM MgSO<sub>4</sub>) and on CYE 1.5 or 0.5% Agar plates at 32°C. When necessary, the following antibiotics were added to the media at the indicated concentrations: kanamycin, 50 or 200 µg/ml; and ampicillin, 100 µg/ml. The inducible promoters P<sub>BAD</sub> and P<sub>lac</sub> were induced with Arabinose at 0.2% and IPTG at 1 mM respectively.

### Motility phenotypic assay

For motility phenotypic assays, exponentially growing cells in CYE medium at 32°C were adjusted to an OD<sub>600</sub> of 5 in TPM buffer and

spotted (5 µl) on CYE plates containing an agar concentration of 0.5% (soft) or 1.5% (hard), incubated at 32°C and photographed after 48–72 h with an Olympus SZ61.

### Microscopy and image analysis

For standard microscopy, *M. xanthus* or *E. coli* cells, exponentially growing cells grown in CYE or LB media, respectively, were washed, concentrated in TPM buffer and mounted on microscope slides covered with a 1.5% TPM agarose pad. The cells were imaged on an automated and inverted epifluorescence microscope TiE-PFS (Nikon), with a 100 × NA = 1.45 Phase Contrast objective and a camera orca flash 4 (Hamamatsu) at room temperature. Mercury fluorescent lamp with green and red optical filters was used when necessary. Images analysis, pictures and movies were prepared for publication using Fiji (<https://fiji.sc/>) and Adobe Photoshop. All images presented in the Figures and Figures EV are representative of three biological replicates.

### Protein production and purification

Plasmids expressing His<sub>6</sub>-tagged FrzS<sup>CheY</sup>, FrzS<sup>CheY</sup> point mutants and Strep-tagged SgmX constructs were transformed into *E. coli* BL21 (DE3). SgmX production and purification have been performed as previously described (Potapova *et al*, 2020). <sup>15</sup>N-labelled FrzS<sup>CheY</sup> and FrzS<sup>CheY</sup> point mutant proteins were produced by growing the cells at 37°C in M9 minimal medium containing 1 g/l of <sup>15</sup>NH<sub>4</sub>Cl as the sole source of nitrogen. The cells were grown at 37°C with shaking until OD<sub>600nm</sub> = 0.7 and protein overexpression was induced by the addition of 1 mM isopropyl-β-D-thiogalactopyranoside (IPTG) followed by incubation for 3 h at 37°C. After centrifugation, cell pellets were suspended in 50 mM Tris–HCl (pH 8.0), 150 mM NaCl, 5 mM MgCl<sub>2</sub> and 20 mM imidazole supplemented with 10 mg/ml of DNase I and EDTA-free protease inhibitor (Roche). Cells were lysed using an Emulsiflex-C5 instrument (Avestin) and clarified by ultracentrifugation for 30 min at 35,000 g. Cell extract containing His<sub>6</sub>-FrzS<sup>CheY</sup> was loaded onto a 1 ml HisTrap HP (Cytiva) column on an Äkta Pure system (Cytiva) equilibrated in affinity buffer (50 mM Tris–HCl (pH 8.0), 150 mM NaCl, 5 mM MgCl<sub>2</sub> and 20 mM Imidazole). His<sub>6</sub>-FrzS<sup>CheY</sup> and FrzS<sup>CheY</sup> point mutants were further purified by size exclusion chromatography using a Superdex-75 Increase column (Cytiva) equilibrated with NMR buffer (50 mM Tris, pH 7.2, 150 mM NaCl and 5 mM MgCl<sub>2</sub>). Purified protein was concentrated using a Vivaspinn-20 cut-off 3 kDa concentrator (Sartorius) to a final concentration of 500 µM.

### NMR spectroscopy

All NMR experiments have been recorded on a 600 MHz Bruker™ AVANCE III spectrometer equipped with a TCI cryoprobe at 298 K. The FrzS<sup>CheY</sup> backbone assignment was carried out by recording 3D HNCO, HN(CA)CO, HN(CO)CA, HNCA, CBCA(CO)NH and HNCACB experiments. The secondary structures were verified based on H<sup>N</sup>, N, C', C<sup>α</sup> and C<sup>β</sup> backbone chemical shifts using TALOS+ webserver (Shen *et al*, 2009). The data were processed using Topspin3.6 (Bruker) and analysed with CCPNMR (Vranken *et al*, 2005).

The FrzS<sup>CheY</sup>/SgmX interaction has been evidenced and characterized using a series of 2D <sup>1</sup>H, <sup>15</sup>N HSQC NMR spectra recorded on a sample of purified <sup>15</sup>N-labelled FrzS<sup>CheY</sup> at 100 μM concentration in the presence of 0.2 molar equivalent of SgmX.

The chemical shift variations for each resonance were calculated using the equation:  $\Delta\delta_{\text{obs}} = [\Delta\delta_{\text{HN}}^2 + (\Delta\delta_{\text{N}}^2/25)]^{1/2}$ , where  $\Delta\delta_{\text{HN}}$  and  $\Delta\delta_{\text{N}}$  are, respectively, the proton and nitrogen chemical shift variations of each residue.

## Data availability

All data porting this study are included in the main text, EV Figures and Appendix.

**Expanded View** for this article is available [online](#).

## Acknowledgements

We thank Olivier Bornet (NMR platform of the Mediterranean Institute of Microbiology, FR 3479 Marseille) for 3D NMR experiments acquisition and processing. This work was funded by the Centre National de la Recherche Scientifique (CNRS), Aix-Marseille University, the European Research Council to TM (JAWS-Advanced Grant ERC-2019-ADG: 885145) and The Agence Nationale de la Recherche to RM and LE (PILACT-AAPG-2022: 259552).

## Author contributions

**Sarah Bautista:** Data curation. **Victoria Schmidt:** Data curation. **Annick Guiseppi:** Data curation. **Emilia MF Mauriello:** Conceptualization. **Bouchra Attia:** Data curation. **Latifa Elantak:** Conceptualization; formal analysis; supervision; writing – original draft; writing – review and editing. **Tâm Mignot:** Conceptualization; funding acquisition; writing – original draft; project administration; writing – review and editing. **Romain Mercier:** Conceptualization; data curation; formal analysis; methodology; writing – original draft; project administration; writing – review and editing.

## Disclosure and competing interests statement

The authors declare that they have no conflict of interest.

## References

- Adams DW, Stutzmann S, Stoudmann C, Blokesch M (2019) DNA-uptake pili of *Vibrio cholerae* are required for chitin colonization and capable of kin recognition via sequence-specific self-interaction. *Nat Microbiol* 4: 1545–1557
- Al-Bassam MM, Bibb MJ, Bush MJ, Chandra G, Buttner MJ (2014) Response regulator heterodimer formation controls a key stage in *Streptomyces* development. *PLoS Genet* 10: e1004554
- Berry JL, Pelicic V (2015) Exceptionally widespread nanomachines composed of type IV pili: the prokaryotic Swiss Army knives. *FEMS Microbiol Rev* 39: 134–154
- Bhaya D, Bianco NR, Bryant D, Grossman A (2000) Type IV pilus biogenesis and motility in the cyanobacterium *Synechocystis* sp. PCC6803. *Mol Microbiol* 37: 941–951
- Bourret RB (2010) Receiver domain structure and function in response regulator proteins. *Curr Opin Microbiol* 13: 142–149
- Bulyha I, Schmidt C, Lenz P, Jakovljevic V, Hone A, Maier B, Hoppert M, Sogaard-Andersen L (2009) Regulation of the type IV pili molecular machine by dynamic localization of two motor proteins. *Mol Microbiol* 74: 691–706
- Bustamante VH, Martinez-Flores I, Vlamakis HC, Zusman DR (2004) Analysis of the Frz signal transduction system of *Myxococcus xanthus* shows the importance of the conserved C-terminal region of the cytoplasmic chemoreceptor FrzCD in sensing signals. *Mol Microbiol* 53: 1501–1513
- Carter T, Buensuceso RN, Tammam S, Lamers RP, Harvey H, Howell PL, Burrows LL (2017) The type IVa pilus machinery is recruited to sites of future cell division. *mBio* 8: e02103-16
- Chang YW, Rettberg LA, Treuner-Lange A, Iwasa J, Sogaard-Andersen L, Jensen GJ (2016) Architecture of the type IVa pilus machine. *Science* 351: aad2001
- Chang YW, Kjaer A, Ortega DR, Kovacicova G, Sutherland JA, Rettberg LA, Taylor RK, Jensen GJ (2017) Architecture of the *Vibrio cholerae* toxin-coregulated pilus machine revealed by electron cryotomography. *Nat Microbiol* 2: 16269
- Collins MJ, Childers WS (2021) The upcycled roles of pseudoenzymes in two-component signal transduction. *Curr Opin Microbiol* 61: 82–90
- Desai SK, Kenney LJ (2017) To ~P or Not to ~P? Non-canonical activation by two-component response regulators. *Mol Microbiol* 103: 203–213
- Faure LM, Fiche JB, Espinosa L, Ducret A, Anantharaman V, Luciano J, Lhospice S, Islam ST, Treguier J, Sotes M et al (2016) The mechanism of force transmission at bacterial focal adhesion complexes. *Nature* 539: 530–535
- Fraser JS, Merlie JP Jr, Echols N, Weisfield SR, Mignot T, Wemmer DE, Zusman DR, Alber T (2007) An atypical receiver domain controls the dynamic polar localization of the *Myxococcus xanthus* social motility protein FrzS. *Mol Microbiol* 65: 319–332
- Fu G, Bandaria JN, Le Gall AV, Fan X, Yildiz A, Mignot T, Zusman DR, Nan B (2018) MotAB-like machinery drives the movement of MreB filaments during bacterial gliding motility. *Proc Natl Acad Sci USA* 115: 2484–2489
- Gao R, Stock AM (2010) Molecular strategies for phosphorylation-mediated regulation of response regulator activity. *Curr Opin Microbiol* 13: 160–167
- Gao R, Bouillet S, Stock AM (2019) Structural basis of response regulator function. *Annu Rev Microbiol* 73: 175–197
- Giltner CL, Nguyen Y, Burrows LL (2012) Type IV pilin proteins: versatile molecular modules. *Microbiol Mol Biol Rev* 76: 740–772
- Gloag ES, Turnbull L, Huang A, Vallotton P, Wang H, Nolan LM, Mililli L, Hunt C, Lu J, Osvath SR et al (2013) Self-organization of bacterial biofilms is facilitated by extracellular DNA. *Proc Natl Acad Sci USA* 110: 11541–11546
- Gloag ES, Turnbull L, Javed MA, Wang H, Gee ML, Wade SA, Whitchurch CB (2016) Stigmergy co-ordinates multicellular collective behaviours during *Myxococcus xanthus* surface migration. *Sci Rep* 6: 26005
- Gold VA, Salzer R, Averhoff B, Kuhlbrandt W (2015) Structure of a type IV pilus machinery in the open and closed state. *eLife* 4: e07380
- Guzzo M, Agrebi R, Espinosa L, Baronian G, Molle V, Mauriello EM, Brochier-Armanet C, Mignot T (2015) Evolution and design governing signal precision and amplification in a bacterial chemosensory pathway. *PLoS Genet* 11: e1005460
- Guzzo M, Murray SM, Martineau E, Lhospice S, Baronian G, My L, Zhang Y, Espinosa L, Vincentelli R, Bratton BP et al (2018) A gated relaxation oscillator mediated by FrzX controls morphogenetic movements in *Myxococcus xanthus*. *Nat Microbiol* 3: 948–959
- Kaczmarczyk A, Hempel AM, von Arx C, Böhm R, Dubey BN, Nesper J, Schirmer T, Hiller S, Jenal U (2020) Precise timing of transcription by c-di-GMP coordinates cell cycle and morphogenesis in *Caulobacter*. *Nat Commun* 11: 816

- Lenarcic R, Halbedel S, Visser L, Shaw M, Wu LJ, Errington J, Marenduzzo D, Hamoen LW (2009) Localisation of DivIVA by targeting to negatively curved membranes. *EMBO J* 28: 2272–2282
- Leonardy S, Miertzschke M, Bulyha I, Sperling E, Wittinghofer A, Sogaard-Andersen L (2010) Regulation of dynamic polarity switching in bacteria by a Ras-like G-protein and its cognate GAP. *EMBO J* 29: 2276–2289
- Lim HC, Bernhardt TG (2019) A PopZ-linked apical recruitment assay for studying protein-protein interactions in the bacterial cell envelope. *Mol Microbiol* 112: 1757–1768
- Maule AF, Wright DP, Weiner JJ, Han L, Peterson FC, Volkman BF, Silvaggi NR, Ulijasz AT (2015) The aspartate-less receiver (ALR) domains: distribution, structure and function. *PLoS Pathog* 11: e1004795
- Mercier R, Mignot T (2016) Regulations governing the multicellular lifestyle of *Myxococcus xanthus*. *Curr Opin Microbiol* 34: 104–110
- Mercier R, Bautista S, Delannoy M, Gibert M, Guiseppi A, Herrou J, Mauriello EMF, Mignot T (2020) The polar Ras-like GTPase MglA activates type IV pilus via SgmX to enable twitching motility in *Myxococcus xanthus*. *Proc Natl Acad Sci USA* 117: 28366–28373
- Mignot T, Merlie JP Jr, Zusman DR (2007) Two localization motifs mediate polar residence of FrzS during cell movement and reversals of *Myxococcus xanthus*. *Mol Microbiol* 65: 363–372
- Nakane D, Nishizaka T (2017) Asymmetric distribution of type IV pili triggered by directional light in unicellular cyanobacteria. *Proc Natl Acad Sci USA* 114: 6593–6598
- Oliva MA, Halbedel S, Freund SM, Dutow P, Leonard TA, Veprintsev DB, Hamoen LW, Löwe J (2010) Features critical for membrane binding revealed by DivIVA crystal structure. *EMBO J* 29: 1988–2001
- Perez-Riba A, Itzhaki LS (2019) The tetratricopeptide-repeat motif is a versatile platform that enables diverse modes of molecular recognition. *Curr Opin Struct Biol* 54: 43–49
- Potapova A, Carreira LAM, Sogaard-Andersen L (2020) The small GTPase MglA together with the TPR domain protein SgmX stimulates type IV pili formation in *M. xanthus*. *Proc Natl Acad Sci USA* 117: 23859–23868
- Sambrook J, Fritsch EF, Maniatis T (1989) *Molecular cloning: a laboratory manual*. Cold Spring Harbor, NY: Cold Spring Harbor Laboratory Press
- Shen Y, Delaglio F, Cornilescu G, Bax A (2009) TALOS+: a hybrid method for predicting protein backbone torsion angles from NMR chemical shifts. *J Biomol NMR* 44: 213–223
- Skerker JM, Berg HC (2001) Direct observation of extension and retraction of type IV pili. *Proc Natl Acad Sci USA* 98: 6901–6904
- Sun H, Zusman DR, Shi W (2000) Type IV pilus of *Myxococcus xanthus* is a motility apparatus controlled by the frz chemosensory system. *Curr Biol* 10: 1143–1146
- Szadkowski D, Harms A, Carreira LAM, Wigbers M, Potapova A, Wuichet K, Keilberg D, Gerland U, Sogaard-Andersen L (2019) Spatial control of the GTPase MglA by localized RomR-RomX GEF and MglB GAP activities enables *Myxococcus xanthus* motility. *Nat Microbiol* 4: 1344–1355
- Tala L, Fineberg A, Kukura P, Persat A (2019) *Pseudomonas aeruginosa* orchestrates twitching motility by sequential control of type IV pili movements. *Nat Microbiol* 4: 774–780
- Treuner-Lange A, Macia E, Guzzo M, Hot E, Faure LM, Jakobczak B, Espinosa L, Alcor D, Ducret A, Keilberg D et al (2015) The small G-protein MglA connects to the MreB actin cytoskeleton at bacterial focal adhesions. *J Cell Biol* 210: 243–256
- Vranken WF, Boucher W, Stevens TJ, Fogh RH, Pajon A, Llinas M, Ulrich EL, Markley JL, Ionides J, Laue ED (2005) The CCPN data model for NMR spectroscopy: development of a software pipeline. *Proteins* 59: 687–696
- Ward MJ, Lew H, Zusman DR (2000) Social motility in *Myxococcus xanthus* requires FrzS, a protein with an extensive coiled-coil domain. *Mol Microbiol* 37: 1357–1371
- Yang R, Bartle S, Otto R, Stassinopoulos A, Rogers M, Plamann L, Hartzell P (2004) AglZ is a filament-forming coiled-coil protein required for adventurous gliding motility of *Myxococcus xanthus*. *J Bacteriol* 186: 6168–6178
- Zhang Y, Franco M, Ducret A, Mignot T (2010) A bacterial Ras-like small GTP-binding protein and its cognate GAP establish a dynamic spatial polarity axis to control directed motility. *PLoS Biol* 8: e1000430
- Zhang Y, Guzzo M, Ducret A, Li YZ, Mignot T (2012) A dynamic response regulator protein modulates G-protein-dependent polarity in the bacterium *Myxococcus xanthus*. *PLoS Genet* 8: e1002872



**License:** This is an open access article under the terms of the [Creative Commons Attribution-NonCommercial-NoDerivs](https://creativecommons.org/licenses/by-nc-nd/4.0/) License, which permits use and distribution in any medium, provided the original work is properly cited, the use is non-commercial and no modifications or adaptations are made.